JACC Vol. 30, No. 6
November 15, 1997:1562–74

Hemodynamic Determinants of Doppler Pulmonary Venous Flow Velocity Components: New Insights From Studies in Lightly Sedated Normal Dogs

CHRISTOPHER P. APPLETON, MD, FACC

Scottsdale, Arizona

Objectives. **We sought to define the hemodynamic determinants of pulmonary venous (PV) flow velocities to assess how these are affected by respiration, heart rate and loading conditions.**

Background. **Pulmonary venous flow velocity (PVFV) recorded with pulsed wave Doppler technique is currently used in the noninvasive evaluation of left ventricular (LV) diastolic function and filling pressures. Although previous studies in both animals and humans have shown that PV flow is pulsatile, the hemodynamic determinants of the individual components of this flow remain controversial. Understanding the physiologic mechanisms should help to better define the clinical utility of these Doppler techniques.**

Methods. **PV flow velocities obtained with transesophageal pulsed wave Doppler imaging were recorded together with PV, left atrial (LA) and LV pressures in 10 sedated, spontaneously breathing normal dogs. PVFV and hemodynamic data were analyzed during apnea, inspiration and expiration, at atrial paced heart rates of 60, 80, 100 and 120 beats/min and mean LA pressures of 6, 12, 18 and 24 mm Hg.**

Results. **The data showed that 1) PV pressure varied depending on recording site, resembling pulmonary artery pressure closer to the pulmonary capillary bed and LA pressure closer to the venoatrial junction; 2) PVFV qualitatively followed changes in the PV–LA pressure gradient; 3) four PVFV components exist under normal conditions—three of which follow phasic changes in LA pressure and one of which (the late systolic component) is more influenced by RV stroke volume and the compliance of the pulmonary veins and left atrium; 4) normal respiration and changes in heart rate significantly alter PVFV variables—in particular, reverse flow velocity at atrial contraction; and 5) increasing LA pressure results in larger PV A wave and PV early systolic flow velocities, as well as an earlier peak in PV late systolic flow velocity and a more prominent velocity minimum before PV diastolic flow.**

Conclusions. **Using transesophageal pulsed wave Doppler technique, four PVFV components are identifiable and determined by PV–LA hemodynamic pressure gradients. These gradients appear to be influenced by a combination of physiologic events that include RV stroke volume, the compliance of the pulmonary vasculature and left atrium and phasic changes in LA pressure. PV flow velocity components are significantly influenced by heart rate, respiration and LA pressure. These findings have implications for the interpretation of LV diastolic function and filling pressures by current Doppler echocardiographic techniques but require further clinical investigation.**

(J Am Coll Cardiol 1997;30:1562–74)

Nearly 40 years ago, work by Lee and Dubois (1) suggested that blood flow through the pulmonary capillary vessels is pulsatile. Since then, mathematic models (2–4) and multiple studies using different techniques in both animals (6–15) and humans (16–18) have confirmed the phasic nature of pulmonary venous (PV) flow. However, the physiologic determinants of the pulsatility have remained controversial. Some investigators have attributed PV flow to forward transmission of pressure pulses from the right ventricle (RV) (2–6), whereas others have seemingly demonstrated an inverse relation between flow and phasic left atrial (LA) pressure (10–20).

More recently, interest in analyzing PV flow has been renewed using Doppler echocardiography (21–25). Clinical studies have been performed in normal subjects (21,23,24,26–31) and in patients with various cardiac diseases (21–23,25,28,32–41). These studies suggest that PV diastolic flow follows the events of left ventricular (LV) filling (21,32,34,35) and that PV systolic flow is influenced by LA size, contractility and compliance (22,34,39). In conjunction with mitral flow velocity, pulmonary venous flow velocity (PVFV) is used to help indirectly assess LV diastolic function (41,42) and LV filling pressures (32–34,36–40). Although these results are encouraging, PVFV variables are age dependent (26–31), and opposite findings to those observed in clinical studies can be seen in normal experimental animals that demonstrate atrial preload reserve (10,12,43,44). Therefore, a better understanding of the fundamental hemodynamic determinants of PV flow

From the Cardiovascular Section, Mayo Clinic Arizona, Scottsdale, Arizona. This study was supported in part by Grant 5-083 from the Arizona Disease Research Commission and by the Arizona Affiliate of the American Heart Association, Phoenix, Arizona.

Manuscript received October 8, 1996; revised manuscript received July 28, 1997, accepted August 14, 1997.

Address for correspondence: Dr. Christopher Appleton, Cardiovascular Diseases, 3A, 13400 East Shea Boulevard, Scottsdale, Arizona 85259.

Published by Elsevier Science Inc.

0735-1097/97/$17.00
PII S0735-1097(97)00354-9

Abbreviations and Acronyms

ECG = electrocardiogram
LA = left atrium, left atrial
LV = left ventricle, left ventricular
PV = pulmonary venous
PVFV = pulmonary venous flow velocity
PVa = reverse pulmonary venous flow velocity at atrial contraction
PVd = pulmonary venous flow velocity in early diastole
PVs1 = pulmonary venous flow velocity in early systole
PVs2 = pulmonary venous flow velocity in late systole
RV = right ventricle, right ventricular

seems necessary to better define the usefulness and limitations of these newly described Doppler variables in predicting LV filling pressures.

Accordingly, using a combination of pulsed wave Doppler echocardiography and simultaneous recording of PV, LA and LV pressures, PVFV and its relation to these hemodynamic data were studied in 10 lightly sedated, spontaneously breathing normal dogs. The effect of normal respiration, different heart rates and increasing LA pressure on PV hemodynamic data and PVFV variables were individually examined.

Methods

Surgical preparation. Ten mongrel dogs (weight 15 to 25 kg) were anesthetized with isoflurane gas, and using sterile technique, a left thoracotomy was performed in the fifth intercostal space. A small incision was made in the pericardium, and 8F Silastic catheters were placed 1 to 2 cm into the LA through stab wound incisions in the LA body and appendage. The pericardium was reapproximated and sutured. A third Silastic catheter was then positioned into the right pleural space. The catheters were filled with heparin and tunneled subcutaneously to an area over the left lateral chest wall. The muscle, subcutaneous tissue and skin were closed in layers. The animals were allowed to recover for a minimum of 3 days before study.

Protocol instrumentation and calibration. On the day of the experiment, the animals were sedated with diazepam (0.5 mg/kg body weight) and hydromorphone (0.3 mg/kg) and then anesthetized with isoflurane while undergoing instrumentation. A 7F dual-sensor (4 cm apart) micromanometer-tipped catheter with fluid-filled reference lumen (Millar Instruments) was inserted into the LV through the left femoral artery. A similar catheter was inserted into the RV through the right internal jugular vein. PV and LA pressures were obtained by passing two 4F micromanometer-tipped catheters retrograde through the LA Silastic tubes. Intrathoracic pressure was recorded with a 5F micromanometer-tipped catheter in the pleural space. A 5F bipolar pacing wire was positioned in the right atrial appendage through the right external jugular vein. A pulmonary artery catheter was placed through the right external jugular vein for cardiac output measurement. After instrumentation, anesthesia was discontinued and the animals were allowed to recover for 30 min before the start of the protocol. Further sedation was provided as necessary with a 2:1 mixture of hydromorphone/diazepam in doses of 0.01 to 0.05 mg/kg.

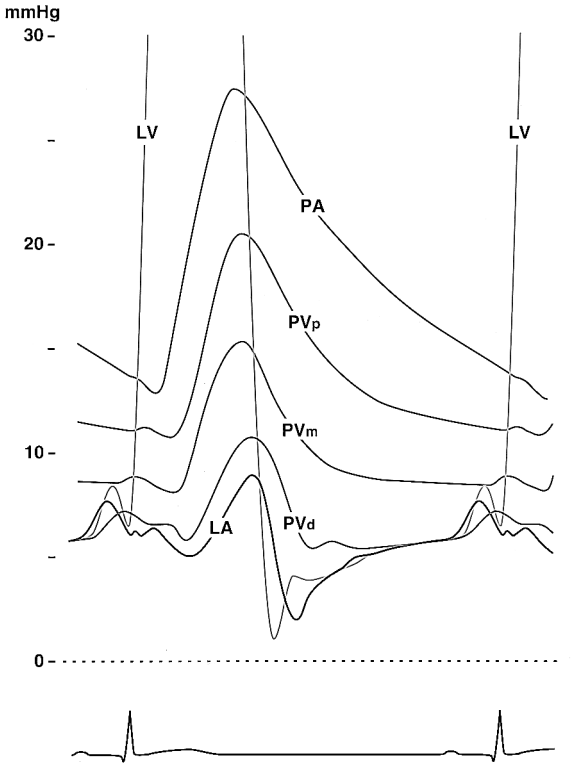

Figure 1. Left ventricular (LV), left atrial (LA), pulmonary artery (PA) and "family" of pulmonary venous (PVp, PVm, PVd) pressures from one dog. The LV and PV pressures are from micromanometer-tipped pressure catheters, whereas the PA pressure is recorded with a fluid-filled catheter, which delays this recording slightly. The figure is an assembled composite, with the PA, PVp, LV and LA pressures measured simultaneously, and PVm and PVd measured by the pull-back technique (total distance PVp–PVd = 3 to 5 cm). In the pulmonary veins, locations closer to the pulmonary venules and capillary bed (PVp) showed the highest pressures, with a contour resembling PA pressure. Recordings closer to the LA (PVm, PVd) showed lower systolic and diastolic pressures and contours more like LA pressure. The magnitude of A and C waves gradually decreased and started later at sites farther back into the PV, suggesting that they originated in the LA. In contrast, the progressively later timing of the peak PV late systolic and LA pressures suggests that these are generated by RV stroke volume.

Zero reference for the micromanometer-tipped catheters was obtained by immersing them in body temperature saline for 60 min before insertion, at a height equal to 50%, of the transthoracic diameter of the animal's chest. After insertion, zero pressure reference was provided by the fluid-filled lumen of the LV catheter. The late diastolic (pre-atrial contraction) pressure waveforms from the LV micromanometer were adjusted to match the comparable fluid-filled pressure recording on cardiac cycles with RR intervals >1,000 ms (43). The LA and PV pressures were then matched to the high fidelity LV

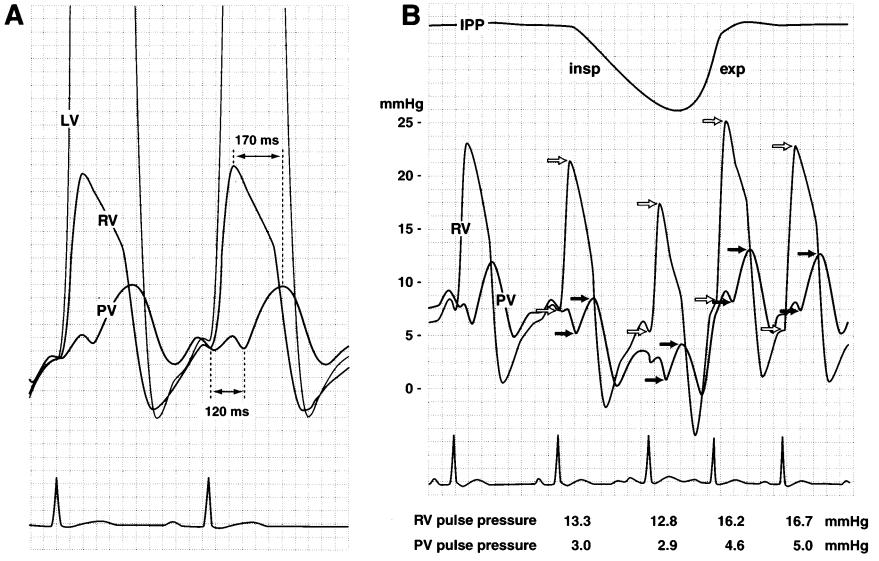

Figure 2. Micromanometer pressure recordings illustrating the timing and pulse amplitude relations between the RV and PV late systolic pressure. **A,** Left ventricular (LV), RV and PV pressures are recorded during apnea. The delay in systolic pressure increase between the RV and PV is 120 ms, with a delay between peak systolic pressures of 170 ms. **B,** Right ventricular, PV and intrapleural (IPP) pressures are recorded during one respiratory cycle. Note the close coupling between RV systolic and PV late systolic pressures, with the respiratory variation in RV pulse pressure (**open arrows**) and ejection time being directly related to changes in PV systolic pulse pressure (**solid arrows**). exp = expiration; insp = inspiration.

pressure recording in a similar fashion. The phase of respiration was determined by changes in intrapleural pressure.

Data gathering and analysis. *Baseline measurements.* At a spontaneous or atrial paced heart rate of 65 to 75 beats/min, hemodynamic and Doppler variables were averaged for three cardiac cycles obtained during apnea. PV pressure was initially recorded as far "upstream" in the PV as possible and then at two sites closer to the LA (total distance 3 to 5 cm) (Fig. 1). The final placement of the catheter was ~2 cm into the PV so as to approximate the same location that pulsed wave Doppler flow velocity was recorded. Right ventricular and PV pressures were simultaneously recorded as shown in Figure 2. Hemodynamic measurements included heart rate, PR interval, mean aortic, PV and LA pressures and maximal values for PV and LA A, C and V waves and LV end-diastolic pressure. Cardiac output was determined in triplicate by the thermodilution technique.

PVFV was obtained using transesophageal imaging and the pulsed wave Doppler technique (CFM 750, Vingmed Inc.) by placing a 2- to 3-mm sample volume 2 cm into the left lower PV. The PVFV variables measured are shown in Figure 3A.

Hemodynamic and Doppler variables during respiration and with changes in heart rate and loading conditions. To assess the effects of normal respiration, the hemodynamic and PVFV variables measured during apnea were compared with those variables obtained during inspiration and expiration. The effects of heart rate were assessed by comparing recordings at heart rates of 60, 80, 100 and 120 beats/min induced with atrial pacing. Finally, the effects of increasing pressure on hemodynamic relations and PVFV were assessed by rapidly infusing a volume expander (Hetastarch) until mean LA pressure was sequentially 12, 18 and 24 mm Hg. In this last circumstance, additional PVFV variables were measured, as shown in Figure 3B.

This protocol was approved by the Animal Research Committees of the Mayo Clinic, Scottsdale. Specific attention was

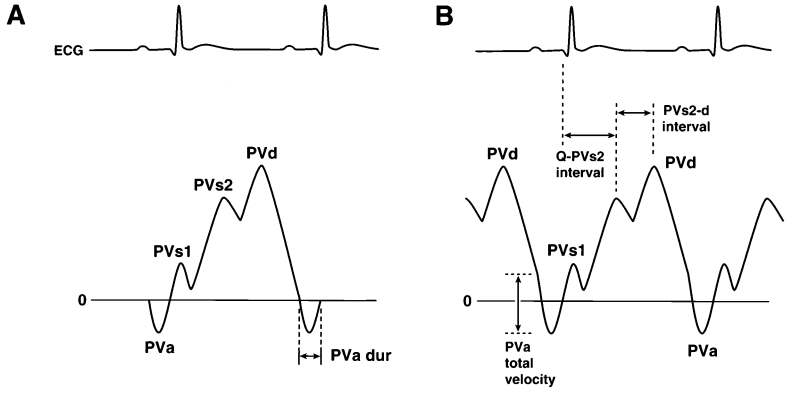

Figure 3. Schematic diagram of PVFV with the electrocardiographic tracing illustrating the Doppler variables measured during different parts of the experiments. **A,** The basic measurements included peak flow velocity in early ventricular systole (PVs1), peak flow velocity in late systole (PVs2), peak diastolic flow velocity (PVd), peak reverse flow velocity at atrial contraction (PVa) and the duration of peak reverse flow velocity at atrial contraction (PVa dur). **B,** Three additional PVFV measurements made when mean LA pressure was increased to 12, 18 and 24 mm Hg. The PVa total velocity measured the entire velocity change that resulted from atrial contraction, regardless of whether PV velocity was positive at the start of atrial contraction (**B**) or at the zero velocity baseline (**A**). The intervals from the start of the QRS complex to peak late systolic PV flow velocity (Q–PVs2 interval) and peak PVs2 velocity (**B**) to peak diastolic flow velocity (PVs2–d interval) were also measured.

Table 1. Hemodynamic and Doppler Pulmonary Venous Flow Velocity Variables in 10 Dogs Under Baseline Rest Conditions

Hemodynamic variable	
Heart rate (beats/min)	68.9 ± 3.2
PR interval (ms)	152 ± 11
Mean aortic pressure (mm Hg)	95.5 ± 9.0
Cardiac output (liter/m)	3.89 ± 0.6
PV pressures (mm Hg)	
Mean	8.5 ± 2.3
Peak A wave	9.0 ± 2.5
Peak C wave	8.2 ± 1.8
Peak V wave	12.7 ± 3.1
LA pressures (mm Hg)	
Mean	7.1 ± 2.3
Peak A wave	10.1 ± 2.3
Peak C wave	8.2 ± 1.8
Peak V wave	11.0 ± 2.9
LVED pressure (mm Hg)	8.2 ± 2.5
PV velocity (cm/s)	
Peak PVs1	22.9 ± 9.1
Peak PVs2	48.5 ± 16.1
Peak PVd	64.0 ± 20.4
Peak PVa	18.3 ± 3.6
PVa duration (ms)	114.2 ± 18.6
PV VT integral (cm)	
PVs1 VTI	2.96 ± 1.10
PVs2 VTI	9.29 ± 2.68
PVd VTI	14.60 ± 3.74
PVa VTI	1.62 ± 0.67

All data presented are mean value ± SD. LA = left atrial; LVED = left ventricular end-diastolic; PV = pulmonary venous; PVa = peak reverse pulmonary venous flow velocity at atrial contraction; PVa duration = duration of reverse pulmonary venous flow velocity at atrial contraction; PVd, PVs1 and PVs2 = peak pulmonary venous flow velocity in early diastole (D), early systole (s1) and late systole (s2); VTI = velocity–time integral.

given to the appropriateness of the animal model, the adequacy of anesthesia and the methods of instrumentation. This protocol is also in accordance with the "Position of the American Heart Association on Research Animal Use," adopted by the Association in November 1984.

Statistical analysis. Baseline hemodynamic and Doppler variables are expressed as the mean value ± SD. Hemodynamic and Doppler variables after respiration or changes in heart rate or LA pressure are expressed as the mean value ± SEM. Differences between mean values for hemodynamic and Doppler variables during the different phases of respiration, at different heart rates or at different LA pressures, were compared using analysis of variance. When differences between groups were found, the Scheffé F test was performed to determine which groups differed. Correlations between hemodynamic and Doppler variables were performed with linear regression analysis. Significance of all statistical tests was considered at $p < 0.05$.

Results

Baseline conditions. Hemodynamic and Doppler PVFV variables under baseline conditions are shown in Table 1. The heart rate averaged 70 beats/min and mean LA pressure ~7 mm Hg. The PV diastolic flow velocity and velocity–time integrals exceeded their systolic flow velocity counterparts, and PV A wave flow velocity reversals were small, averaging <20 cm/s.

Relation between RV, pulmonary artery and PV and LA pressures. PV pressure and contour varied depending on recording site, so that a "family" of successive pressure curves was seen between the pulmonary artery and LA (Fig. 1). At locations closer to the pulmonary venules and capillary bed, the PV pressure contour resembled a delayed pulmonary artery pressure, with mean pressure reduced by 4 to 5 mm Hg. Recording locations closer to the venoatrial junction had pressure contours more like LA pressure, with noticeable A and C waves. These A and C waves were largest in the atrium and delayed and smaller in proportion to the distance upstream in the pulmonary veins.

The maximal PV pressure occurred in late systole (in conjunction with the peak LA V wave) and appeared closely linked to RV pressure events and pulse pressure throughout the respiratory cycle (Fig. 2). Overall this maximal systolic pressure decreased by one-half to two-thirds, traversing the pulmonary artery and capillary beds, with another 10% to 15% pressure decrease between the PVs and LA.

PV flow velocity components and relation to hemodynamic pressure gradients. Although PV pressure and contour varied with distance from the LA, there was an obvious qualitative relation between the PV–LA pressure gradient and PVFV (Fig. 4 and 5). Two maximal pressure gradients were observed during both ventricular systole and diastole. These corresponded in timing to four PVFV components: PVFV in early systole (PVs1), PVFV in late systole (PVs2), PVFV in early diastole (PVd) and reverse PVFV at atrial contraction (PVa).

Figure 5 explains the hemodynamic determinants of these flows. With the mitral valve closed during systole, the PV–LA vascular reservoir is filled with volume from RV systole. Under rest conditions PV pressure rises more rapidly than LA pressure, so the maximal late systolic pressure gradient and PVs2 occur near the end of systole, just before mitral valve opening (Fig. 4). At higher pressures the rise in PV and LA pressure is more equal, and the maximal pressure gradient and PVs2 occur somewhat earlier (Fig. 5). In this way PVs2 appears to be determined by both RV stroke volume and the relation between PV and LA compliance.

After the PV–LA vascular system reaches maximal volume and pressure in late systole, blood is released more passively throughout the rest of the cardiac cycle in accordance with changes in phasic LA pressure. With mitral valve opening, LA and LV pressures decline rapidly and are followed by a slower decline in PV pressure, with the maximal pressure gradient and PVd occurring at LA pressure minimum. Pulmonary venous flow velocity then gradually diminishes through mid-diastole, with flow stopping as PV and LA pressures become equalized. Atrial contraction then causes LA pressure to increase above a relatively "flat" PV pressure, resulting in reverse PVa. With atrial relaxation this process is reversed, LA pressure declines

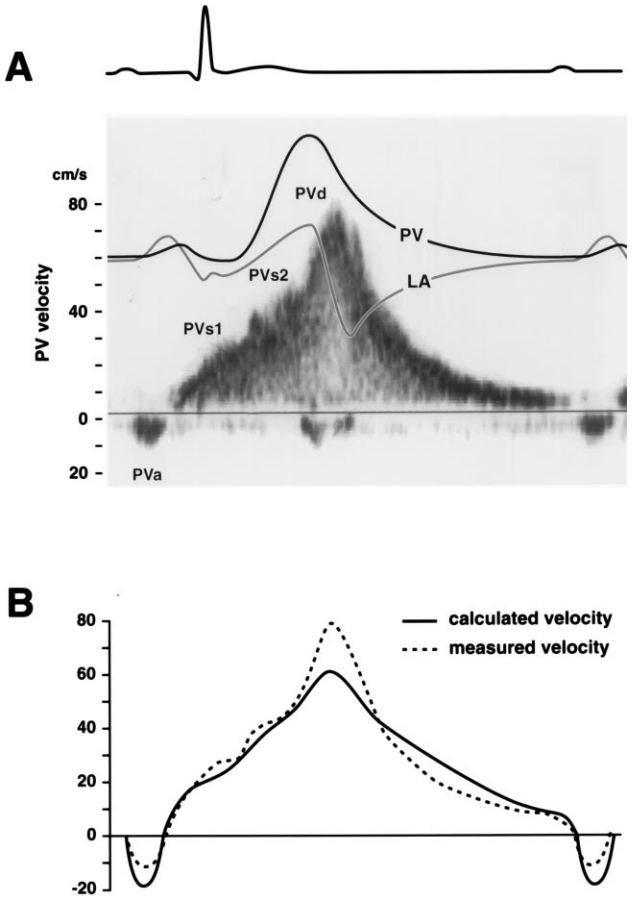

Figure 4. A, Simultaneous recording of PV and LA pressures together with PVFV at a mean LA pressure of ~6 mm Hg. **B,** Schematic drawing compares the measured PVFV (**dashed lines**) with that calculated (**solid line**) using the PV–LA pressure difference and modified Bernoulli equation (Pressure = 4 × Velocity^2). The PVFV components are labeled as in Figure 3.

below PV pressure and forward flow velocity (PVs1) resumes. The peak of both PVa and PVs1 occurs at LA maximal and minimal pressures, respectively. After PVs1 the start of LV contraction and resultant atrial C wave cause a transient decline in PVFV, but almost immediately thereafter RV systolic output reaches the pulmonary veins, late systolic pressure increases and the flow velocity cycle begins again.

The inverse relation between phasic LA pressure and PVFV components was an early observation (18), which has led many investigators to suggest that PV flow was controlled by left heart mechanics. Figure 6 shows that this inverse relation varies depending on the individual flow velocity component and level of filling pressure; at normal pressures maximal flow velocities (and especially PVs2) are more offset in timing than those at higher filling pressures, where there is near concordance of all peak velocities and LA pressure minimums.

Effect of respiration on PVFVs and hemodynamic pressure gradients (Table 2). In general, PVFVs decreased with inspiration and increased on the first two beats of expiration, with the changes most marked for the PVa component (Fig. 7). The respiratory changes in flow velocities were influenced by multiple hemodynamic factors. As intrathoracic pressure varied PV pressure changed more than LA pressure. At the same time respiration also caused changes in RV stroke volume,

Figure 5. A, Simultaneous recording of PVFV together with PV and LA pressures. **B,** Schematic drawing of PV and LA pressures shows the hemodynamic pressure gradients (**hatched areas**) that determine the four individual PVFV components. Reverse PV flow at atrial contraction (PVa) occurs when LA pressure rises with atrial systole and exceeds a PV pressure that is relatively flat (**vertical hatching**). In contrast, PV anterograde flow in early systole (PVs1) is generated when LA pressure falls below PV pressure as a result of atrial relaxation (**horizontal hatching**). The PV diastolic flow velocity (PVd) occurs when the abrupt fall in LV pressure is associated with ventricular relaxation and mitral valve opening. The PVd flow velocity then decreases as PV and LA pressures gradually equilibrate in mid-diastole (**upsloping hatching**). For PVa, PVs1 and PVs2, it appears that changes in phasic LA pressure are the best determinants of these flows. In contrast, PVFV in late systole (PVs2) occurs as a result of the rapid pressure increase in the pulmonary veins associated with RV systole (**downsloping hatching**).

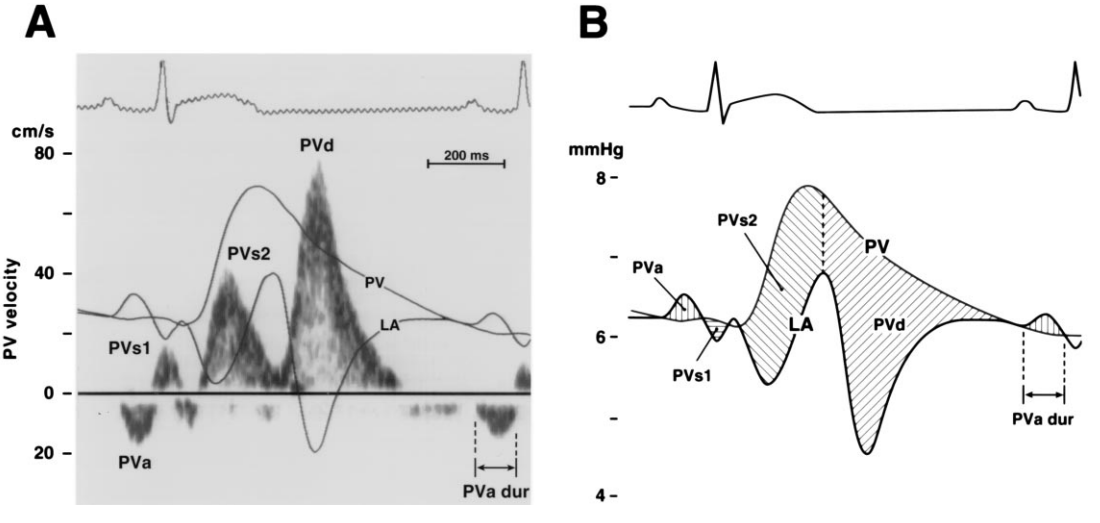

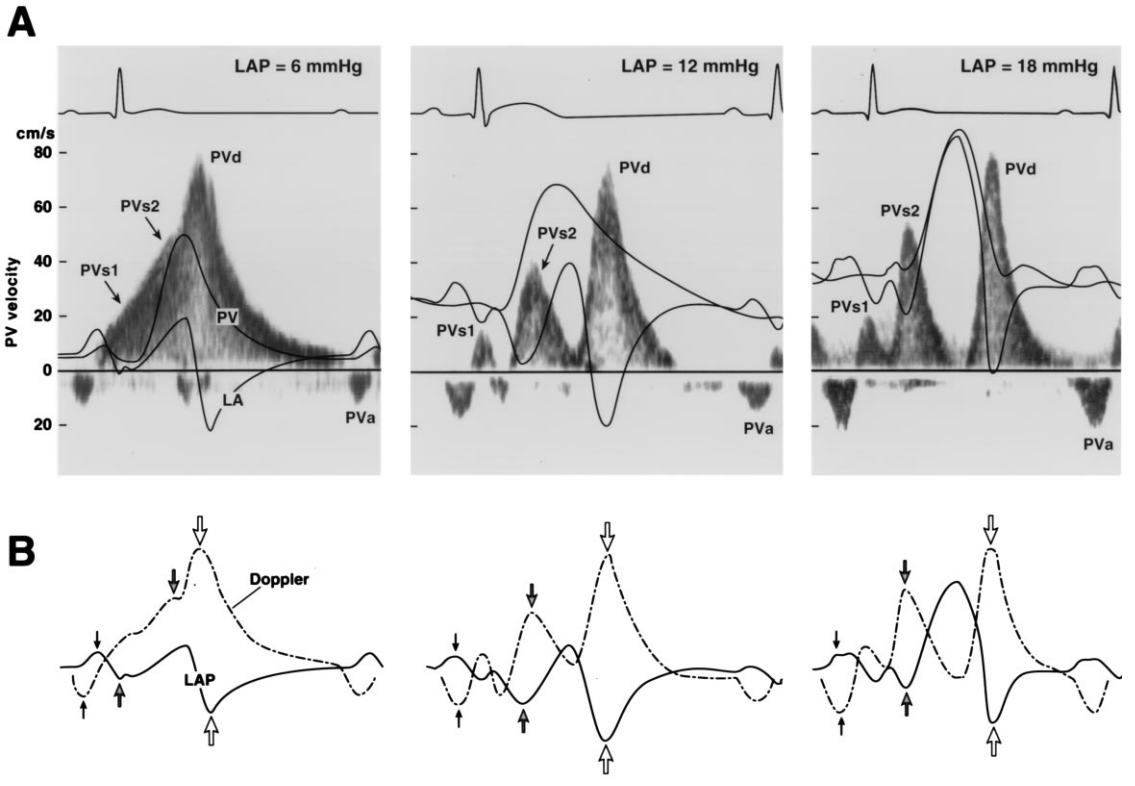

Figure 6. A, PV and LA pressures together with PVFV at increasing LA pressures. **B,** Retracing of Doppler **(dashed lines)** and LA pressure **(solid lines)** shows that the relation of flow velocity peaks and LA pressure minimums **(arrows)** varies depending on pressure level. The PVFV variables are defined as in Figure 3. At lower mean LA pressures (LAP = 6 mm Hg), peak PVd velocity is closely timed with the LA early diastolic pressure minimum **(larger open arrows),** but peak PVa velocity **(small black arrows)** and especially peak PVs2 velocity **(medium gray arrows)** are significantly offset in timing. At 12 mm Hg, the flow velocity peaks and LA pressure minimums match more closely, whereas at 18 mm Hg the inverse timing relation becomes nearly simultaneous.

which altered the PV pulse pressure (Fig. 2), the PV–LA pressure gradient and LA filling and A wave pressure increase. Because the relation between individual cardiac cycles and changes in intrathoracic pressure varied with each respiratory cycle, some variation in flow velocity changes was observed, with the maximal PVa reversal sometimes seen on the second rather than the first beat of expiration. Variation between animals was also observed depending on the relation of the heart rate to respiratory rate. Nevertheless, the basic pattern of lowest flow velocity components on inspiration and highest on expiration was always observed.

Effect of heart rate on PVFVs and hemodynamic pressure gradients. Values for the various Doppler variables at heart rates between 60 and 120 beats/min are shown in Table 3. Changes in heart rate markedly affected PVa and PVs1, with less effect on PVs2 and PVd (Fig. 8). At slower heart rates PV and LA pressures equilibrated in mid-diastole, so that atrial contraction resulted in a reverse pressure gradient and reverse flow back into the PVs. However, at faster heart rates diastole was shortened so that atrial contraction only diminished but did not reverse PV flow. By altering the PVa, faster heart rates also affected PVs1, which increased as the PVa minimum became more positive. PV and LA pressures in late systole and early diastole were less affected by increasing heart rates, explaining the lesser effect on PVs2 and PVd.

Effect of increased filling pressures on PVFVs and velocity intervals. These were somewhat variable depending on each animal, the PVFV component and the level of pressure increase (Table 4). Increasing filling pressures had the largest and most consistent effects on PVa, resulting in both an increase in maximal reverse flow velocity and duration (Fig. 9). Higher pressures also progressively shortened the Q-PVs2 interval, whereas the velocity decrease and separation (gap) between PVs2 and PVd peaks lengthened. The changing relation in PV and LA pressure slopes at different pressures suggests that LA compliance exceeds that of the PV system under normal circumstances, with the reverse being true at elevated filling pressures.

Discussion

Using simultaneous high fidelity pressure recordings of PV and LA pressure together with the pulsed wave Doppler technique, the present study reexamined the hemodynamic origins of PVFV and the effect of changes in several clinical variables in spontaneously breathing dogs. The results reaffirm

Table 2. Respiratory Changes in Hemodynamic and Pulmonary Venous Flow Velocity Variables in the 10 Study Dogs

	Phase of Respiration			
	Apnea	Inspiration	Expiration	Expiration/ Inspiration
Flow velocities				
PVs1 (cm/s)	24.1 ± 2.5	19.5 ± 2.0	26.5 ± 2.5*	7.0 ± 1.5
PVs1 VTI (cm)	1.95 ± 0.26	1.33 ± 0.22	2.53 ± 0.29*	1.20 ± 0.34
PVs2 (cm/s)	51.8 ± 3.2	49.5 ± 3.2	53.5 ± 3.2*	4.0 ± 0.8
PVs2 VTI (cm)	8.95 ± 0.68	8.33 ± 0.52	9.35 ± 0.81*	1.02 ± 0.36
PVd (cm/s)	67.1 ± 3.0	63.9 ± 3.3	72.0 ± 3.5*	8.1 ± 1.2
PVd VTI (cm)	12.99 ± 1.06	11.96 ± 0.86	14.18 ± 1.25*	2.21 ± 0.53
PVa (cm/s)	19.9 ± 1.9	12.9 ± 1.6	24.9 ± 2.3†	12.0 ± 1.9
PVa VTI (cm)	1.62 ± 0.21	1.00 ± 0.21	2.58 ± 0.34†	1.58 ± 0.16
PVa duration (ms)	116.5 ± 9.2	94.2 ± 10.0	140.0 ± 11.0†	46.0 ± 3.8
Pressures				
S1 grad (mm Hg)	2.9 ± 1.7	2.6 ± 1.7	2.9 ± 1.7	0.3 ± 0.1
S2 grad (mm Hg)	4.7 ± 1.4	3.8 ± 1.5	4.8 ± 1.5	0.9 ± 0.3
D grad (mm Hg)	11.3 ± 0.4	10.5 ± 0.2	12.0 ± 0.6*	1.5 ± 0.4
PV A wave grad (mm Hg)	2.0 ± 0.2	0.9 ± 0.5	2.9 ± 0.3*	2.0 ± 0.3
PV A wave (mm Hg)	0.6 ± 0.1	0.4 ± 0.2	0.8 ± 0.1*	0.4 ± 0.1
LA A wave (mm Hg)	2.8 ± 0.3	2.1 ± 0.3	3.5 ± 0.3*	1.4 ± 0.1
LA–PVa dur (ms)	117.5 ± 5.7	79.2 ± 12.4	135.8 ± 8.3†	56.7 ± 7.0

*$p < 0.05$, †$p < 0.01$ compared with inspiratory values. Data presented are mean value ± SEM. S1 grad, S2 grad and D grad = maximal pressure gradient between pulmonary venous and left atrial pressures in early systole (S1), late systole (S2) and early diastole (D); LA A and PV A waves = pressure increase in left atrium and pulmonary vein at atrial contraction; LA–PVa dur = duration of positive pressure gradient between left atrium and pulmonary vein that occurs as a result of atrial contraction; other abbreviations as in Table 1.

many previous observations but also provide new insights into the origins of PVFV components, which helps to resolve old controversies and may also improve the future clinical use of these variables.

PV pressure and relation to pulmonary artery and LA pressures. As shown in Figure 1, PV pressure varies depending on the recording location. At sites nearest the pulmonary capillary bed, the pressure contour resembles that of a delayed pulmonary artery pressure, confirming the assertion of early investigators (4,6) that unlike the systemic circulation, the pulmonary artery pressure pulse and phasic flow traverse the pulmonary resistance vessels without being "damped out." Although never fully explained, this effect may be due to the reduced length of the pulmonary vasculature and a lower vascular resistance. The increase in PV late systolic pressure also occurred progressively later at locations closer to the LA (Fig. 1), confirming cineangiographic evidence (6) that these pressure changes and flow originate from the right heart. The linkage between changes in RV and PV pulse pressure with respiration (Fig. 2) provided further evidence that the late systolic pressure increase in the PV system is a direct result of RV systolic output.

Physiologic events affecting the LA and phasic changes in LA pressure were also found to influence PV hemodynamic data. Figure 1 shows that PV pressure begins to resemble LA pressure in the 2 to 3 cm before the venoatrial junction. Pulmonary venous diastolic pressure follows the rapid decline in LA pressure associated with early diastolic LV filling, and small retrograde pressure pulses are transmitted backward into the PVs at atrial contraction (A wave) and in early ventricular systole (C wave).

Taken together, these results indicate that the PV–LA vascular system is filled with blood by RV stroke volume during mid and late systole when the mitral valve is closed, but then the discharge from this reservoir during diastole and early systole (atrial relaxation) is determined by the events that control phasic LA pressure. In this way, PV flow is regulated by both "upstream" (right heart) and "downstream" (left heart) events depending on the phase of the cardiac cycle.

Determinants of individual PVFV components. Four components (two systolic and two diastolic) were present under normal circumstances and were seen to qualitatively follow the hemodynamic pressure gradients (Fig. 4). Only the late systolic component (PVs2) occurs as a direct result of the right heart filling the PVs and LA. At normal pressures, the late systolic increase in PV was larger and more rapid than in the LA (Fig. 1, 4A and 9A). However, at elevated filling pressures, the late systolic pressure increase in the LA is equal to (Fig. 5) or more rapid (Fig. 9B) than that in the PV, resulting in an earlier maximal pressure gradient and earlier peak PVs2. This suggests that LA compliance exceeds that of the PV reservoir at normal pressures, with the reverse situation at elevated pressures. Therefore, in addition to RV stroke volume, the compliance relation between the pulmonary vasculature and LA appears to determine PVs2 maximum, its timing and flow–velocity integral.

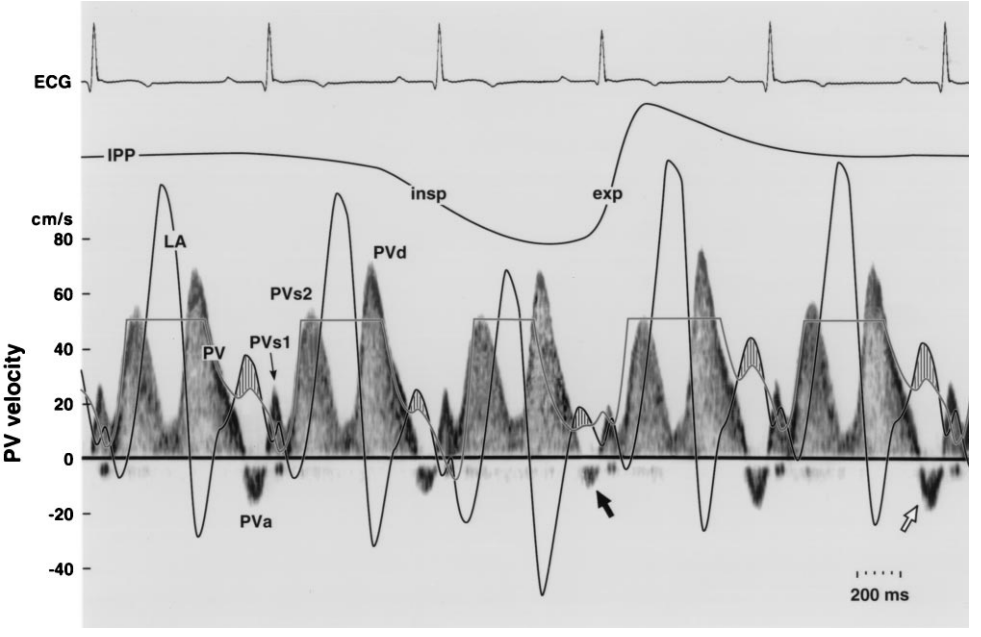

Figure 7. Changes in PV and LA pressures and PVFV during one respiratory cycle. The PVFV components are labeled as in Figure 3. The PV systolic pressure is electronically "clipped" (**horizontal line**) so that maximal late systolic PV–LA pressure gradients cannot be seen in this figure. Compared with apnea (first cardiac cycle), PV and LA pressures decrease on inspiration (insp) and then increase on expiration (exp). The phasic changes in both pressures are not perfectly matched, resulting in a decrease in the PV–LA pressure gradients and flow velocities during inspiration and an increase on expiration. These changes are best seen in the PVa velocity, which decreases to a minimal value during late inspiration (**black arrow**) and increases to a maximum on the first and second (**open arrow**) beats of expiration. The velocity changes are reflected in the PV–LA pressure gradients, as shown by the **hatched lines.** Note how the increase and decrease in LA pressure with atrial contraction changes throughout the respiratory cycle and affects both the PVa and PVs1 flow velocities. IPP = intrapleural pressure.

With the PV–LA reservoir fully charged, the remaining three PVFV components (PVd, PVa and PVs1) followed phasic changes in LA pressure. At normal pressures and rest heart rates, PVd usually continued throughout mid-diastole (Fig. 4). Although low level filling across the mitral valve was also observed, the continued LA filling and larger PV–LA pressure gradient are consistent with studies showing that the LA serves both a reservoir as well as conduit function in mid-diastole at slower heart rates (13,15,44).

As a result of changes in LA pressure due to atrial contraction and relaxation at a time when PV pressure was relatively constant, PVa and PVs1 also occurred (Fig. 5). At slower heart rates the magnitude of LA pressure increase and fall tended to parallel each other, with PVa and PVs1 maximal

Table 3. Changes in Doppler Pulmonary Venous Flow Velocity Variables With Changes in Heart Rate in the 10 Study Dogs

	Heart Rate (beats/min)			
Flow Velocities	60	80	100	120
PVs1 (cm/s)	20.2 ± 3.5	21.6 ± 4.0	30.5 ± 4.5*	46.9 ± 4.3*
PVs1 VTI (cm)	2.49 ± 0.94	3.00 ± 1.21	4.35 ± 1.01†	7.72 ± 1.50†
PVs2 (cm/s)	39.7 ± 5.9	36.2 ± 5.2	35.6 ± 5.8	43.7 ± 5.6
PVs2 VTI (cm)	7.57 ± 1.69	7.20 ± 1.65	6.97 ± 1.73	7.51 ± 1.69
PV sys frac (%)	39.5 ± 2.3	45.5 ± 2.7	50.4 ± 3.4*	69.8 ± 5.1†
PVd (cm/s)	56.5 ± 8.4	52.3 ± 5.3	54.8 ± 4.96	51.1 ± 7.3
PVd VTI (cm)	16.35 ± 4.83	11.77 ± 2.73	9.96 ± 1.99*	6.90 ± 1.92†
PVa (cm/s)	−12.2 ± 1.6	−4.3 ± 2.1*	12.7 ± 1.4†	24.7 ± 1.7†
PVa VTI (cm)	0.98 ± 0.17	0.77 ± 0.33	N/A	N/A
PVa duration (ms)	116.6 ± 6.4	101.0 ± 7.6	N/A	N/A

*$p < 0.05$, †$p < 0.01$ compared with values at 60 beats/min. Data presented are mean value ± SEM. N/A = not applicable; PV sys frac = percent of pulmonary venous forward flow velocity that occurs in systole; other abbreviations as in Tables 1 and 2.

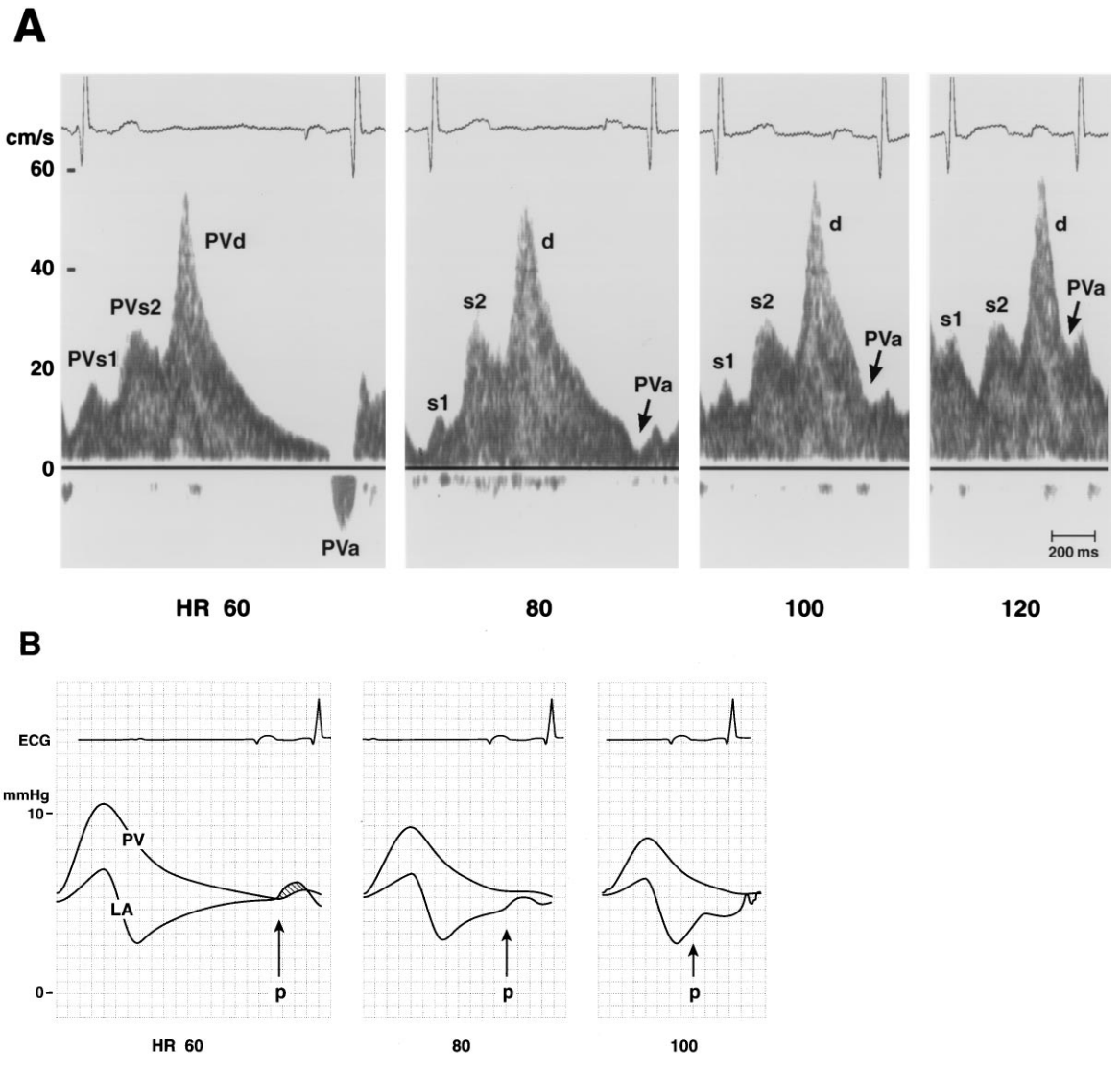

Figure 8. Changes in PVFV (**A**) and PV and LA pressures (**B**) at various heart rates (HR), illustrating how diastolic cycle length and flow velocity at the start of atrial contraction influence PVa and PVs1 flow velocities. The PVFV variables are defined as in Figure 3. At 60 beats/min, PV and LA pressures have sufficient time to equilibrate in mid-diastole so that atrial contraction results in a reverse LA–PV pressure gradient (**B, downsloping hatching**) and retrograde flow velocity (PVa). However, at faster heart rates (80, 100 and 120 beats/min), diastole is shorter, and there remains a positive PV–LA pressure gradient and continued anterograde PVd flow velocity before atrial contraction. In these cases the rise in LA pressure with contraction does not exceed PV pressure, and forward flow velocity is slowed but not reversed **(A, arrows).** The progressive increase in PVa minimal velocity also increases the PVs1 velocity, whereas the relation between PVs2 and PVd remains relatively constant at the various heart rates.

velocities often approximating each other (Fig. 6). At the same time, the A wave pressure increase became both smaller and later in timing in the PV with increasing distance from the LA (Fig. 1). These locational changes in reverse pressure gradient help explain the clinical observation that peak reverse PVa is dependent on pulsed wave Doppler sample volume location in the PV (45,46). With the onset of LV systole, PVs1 decreased in association with the LA C wave, explaining the separation consistently seen between PVs1 and PVs2 velocities in transesophageal Doppler recordings (26,32,33).

Effects of respiration, heart rate and loading conditions. Normal respiration had significant effects on PVFV components, especially peak PVa velocity and duration (Fig. 7). In general, all peak velocities and velocity–time integrals fell during inspiration and increased during expiration. This respiratory variation was influenced by many factors (47), including changes in intrathoracic and intracardiac pressures, changes in RV stroke volume and alterations in LA filling and LA A wave pressure increases. The timing of individual cardiac cycles to phase of respiration, as well as the variability between heart and respiratory rates, introduced additional cycle to cycle variability. Despite all these factors, the expiratory increase in PV pressure was very consistent, presumably because the effect of an increased RV stroke volume from the preceding inspira-

Table 4. Doppler Pulmonary Venous Flow Velocity Variables and Intervals in the 10 Study Dogs at Different Left Atrial Pressures

	Mean Left Atrial Pressure (mm Hg)			
	6	12	18	24
Flow velocities				
PVs1 (cm/s)	33.6 ± 4.9	32.1 ± 3.0	29.4 ± 2.1	36.0 ± 6.1
PVs1 VTI (cm)	4.04 ± 0.60	3.46 ± 0.21	3.20 ± 0.23	2.68 ± 0.24*
PVs2 (cm/s)	49.7 ± 2.6	54.8 ± 2.8	63.1 ± 4.2*	92.8 ± 3.8*
PVs2 VTI (cm)	8.91 ± 0.58	10.40 ± 0.26	12.68 ± 0.99*	14.36 ± 0.82†
PV sys frac (%)	51.8 ± 3.0	55.6 ± 1.0	58.5 ± 1.5*	60.0 ± 2.7*
PVd (cm/s)	63.3 ± 7.0	60.8 ± 4.1	62.2 ± 5.4	80.1 ± 4.9*
PVd VTI (cm)	12.93 ± 1.68	10.76 ± 0.74	11.57 ± 1.37	11.34 ± 0.99
PVa (cm/s)	13.2 ± 7.1	−10.6 ± 1.6*	−20.8 ± 3.1†	−34.2 ± 2.1†
PVa total (cm/s)	19.8 ± 1.8	30.5 ± 1.4*	40.3 ± 2.5†	78.0 ± 3.3†
PVa VTI (cm)	0.48 ± 0.12	0.86 ± 0.16*	1.58 ± 0.32†	2.70 ± 0.29†
PVa dur (ms)	89.0 ± 9.3	97.5 ± 4.8	115.0 ± 4.6*	125.0 ± 4.1*
PVa dur total (ms)	123.3 ± 4.0	154.2 ± 2.4*	164.2 ± 4.2†	166.0 ± 2.5†
Velocity interval				
Q–PVs2 (ms)	285.1 ± 39.6	235.2 ± 18.4*	221.3 ± 18.3*	208.3 ± 31.6*
PVs2–D (ms)	192.5 ± 24.7	273.8 ± 28.6*	303.8 ± 27.9*	310.6 ± 15.6*

*$p < 0.05$, †$p < 0.01$ compared with 6 mm Hg. Data are presented as mean value ± SEM. Other variables are illustrated and defined in Figure 3. Abbreviations as in Tables 1 and 2.

tory beats was additive to the increase in intrathoracic pressure. This resulted in a larger LA pressure increase at atrial contraction and larger peak reverse PVa velocity and duration. The variation between inspiratory and expiratory PVa duration averaged 50 ms, a value large enough to be of clinical relevance if unaccounted for when estimating LV end-diastolic pressures (32,36,37,40).

As shown in Figure 8, heart rate also had a marked effect on PVa and PVs1 velocities, with less effect on PVs2 and PVd components. At slower heart rates, PV and LA pressure equilibrated in mid-diastole, PV flow stopped and atrial contraction then caused retrograde flow back into the PVs. However, at shorter RR intervals, PV and LA pressures had insufficient time for equilibration so that LA contraction only reduced forward flow velocity. Without a flow velocity reversal, PVs1 increased. The heart rate dependency of PVa flow reversal helps explain why PVa reversals are infrequently seen in studies in anesthetized animals (6,11,12–15,18,44) or intraoperative patients (16,18) who have relatively fast heart rates, yet are routinely seen in conscious patients with slower heart rates (26–31,36–40). The influence of heart rate on PVFV variables has been noted in both experimental studies (13,14) and patients with dual-chamber pacemakers (48), whereas in this study the systolic fraction of PV flow increases at faster rates as the diastolic filling period shortens.

As expected, volume loading tended to increase most individual PVFV components. However, as with alterations in respiration and heart rate, increasing filling pressures had the largest effect on increasing peak reverse PVa flow velocity and duration (Fig. 9). Higher LV filling pressures also caused a progressive shortening of the Q–PVs2 interval and an increased separation between PVs2 and PVd velocity peaks. The increase in peak reverse PVa velocity with volume loading was due to a larger increase in LA pressure at atrial contraction. The earlier PVs2 maximum with increasing pressures was likely due to a decrease in LA chamber compliance with a more rapid rise in LA V wave pressure (Fig. 9B).

Comparison with previous studies. The present work largely complements previous experimental and clinical studies by clarifying the hemodynamic origins of the four PVFV components, showing that their origin is influenced by both right heart and left heart physiologic events and providing a basis for understanding some seeming inconsistencies previously reported. For example, studies in animals (15,43) have shown an *increased* systolic fraction of PV flow with volume loading, whereas patients with cardiac disease show a *reduced* PV systolic fraction as filling pressures increase (33,36,38,40). This apparent paradox likely occurs because normal atria and ventricles exhibit preload reserve and increased contractility with volume loading (10,12,13,15,44), whereas abnormal hearts often fail. An increase in LA contractility results in enhanced atrial relaxation, which augments PVs1 velocity. At the same time, increased LV contractility augments LA compliance and PVs2 velocity by increasing LA long-axis dimension in late systole. In contrast, increased pressures in diseased hearts often result in LA and LV systolic failure, a reduction in LA compliance and phasic LA pressure changes and lower PVs1 and PVs2 velocities and PV systolic fraction.

Alterations in PVFV occur with changes in the PR interval (11,13), heart block (22) and atrial fibrillation. Although not specifically studied, the effect of these conduction disturbances on PVFV components are explained by the current results. For instance, with complete heart block, PVa and PVs1 follow atrial contraction and relaxation irrespective of the phase of cardiac cycle (22). Therefore, the terminology of PVs1 as a systolic component may sometimes be inaccurate, as it may

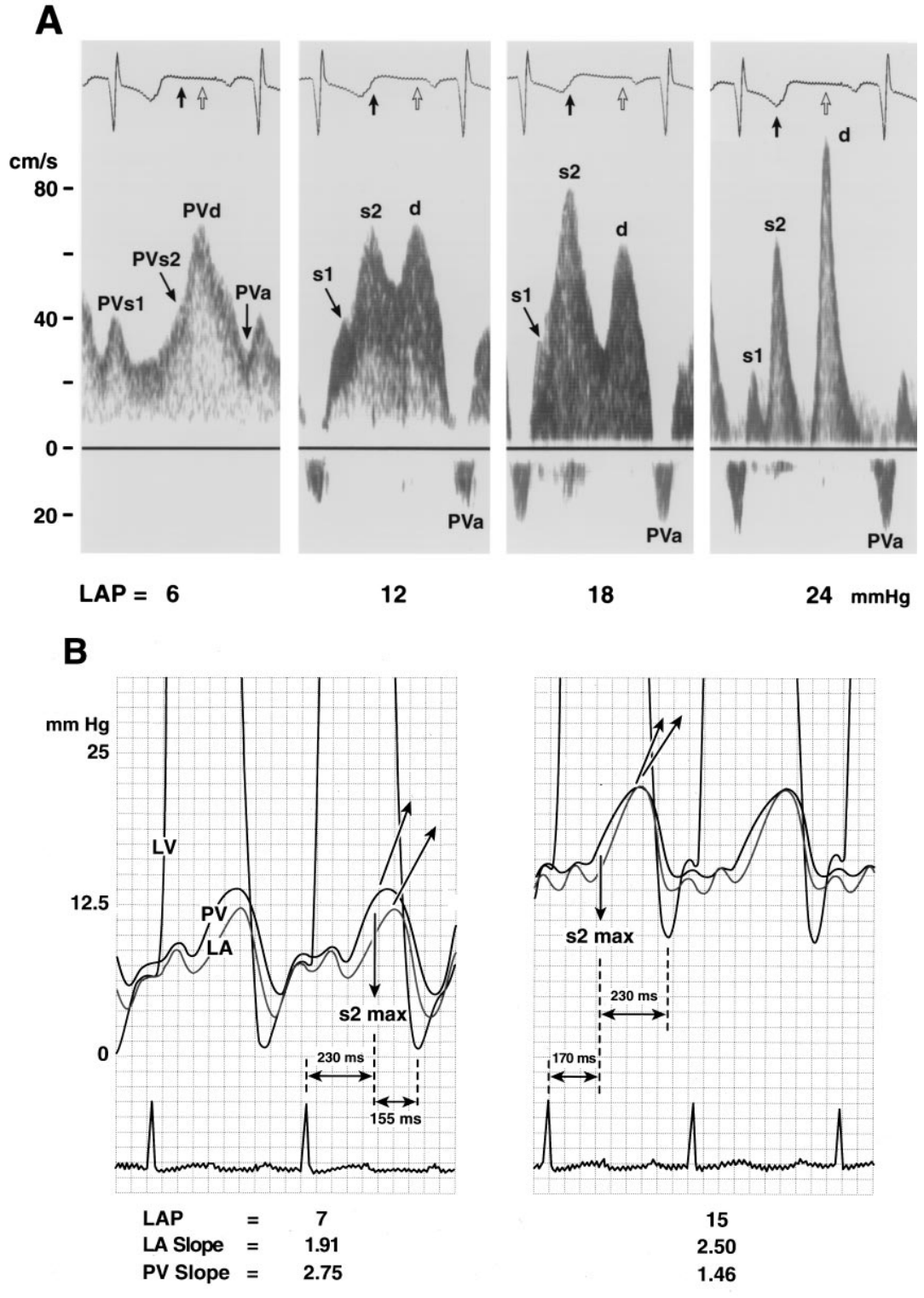

Figure 9. Changes in PVFV (**A**) and PV and LA pressure relations (**B**) at increasing mean LA pressures (LAP). The PVFV variables are defined as in Figure 3. All heart rates in **A** are ~90 to 100 beats/min. Under rest conditions (LAP = 6 mm Hg), there is little separation between peak PVs2 and PVd velocities (**A, first recording and solid and open arrows on the electrocardiogram [ECG]**) and no reversal of flow (PVa) at atrial contraction. **B,** At these normal pressures the PV late systolic pressure rises faster (steeper slope) than LA pressure, so that the maximal pressure gradient that determines PVs2 peak velocity (s2 max) occurs relatively late (230 ms from the peak of the QRS complex). Similarly, the interval from s2 max to peak diastolic pressure gradient is relatively short (155 ms), reflecting the close proximity of PVs2 and PVd flow velocity peaks. At higher LA pressures (12 to 18 mm Hg), reverse PVa velocity appears, PVs2 velocity increases, and the interval between peak PVs2 and PVd velocity widens, with a prominent decrease in velocity between the two peaks (**A, second and third recordings and solid and open arrows on the ECG). B,** At these elevated pressures the late systolic pressure increase in the LA exceeds the PV pressure, resulting in an earlier s2 max pressure gradient (earlier PVs2 velocity peak; **A, solid arrow on the ECG**) and a larger interval between s2 max to peak diastolic maximal pressure gradient (230 ms). At the very highest LA pressure (24 mm Hg), the PVs2 peak velocity continues to move closer to the QRS complex (**solid arrow on the ECG),** although the PVs2–PVd interval actually shortens to 210 ms, probably due to an earlier mitral valve opening.

occur in diastole. Similarly, the timing of PVs1 will change PVs2 maximum by altering the velocity at which it starts. A reduced PVs2 and PV systolic fraction are characteristic of atrial fibrillation, regardless of LV systolic function, where atrial contraction and relaxation are missing altogether. These situations emphasize that PVs2 and PVd are relatively fixed in their timing in the cardiac cycle because of their relation with RV systole and LV relaxation, but the components associated with atrial contraction (PVa) and relaxation (PVs1) are more variable depending on the PR interval, cardiac rhythm and their relation to the systolic phase of the cardiac cycle.

Clinical implications. At present Doppler PVFV variables are used to help estimate LV filling pressures (32–40) and determine if mitral flow velocity patterns are abnormal (41,42,49,50). These methods have so far focused on PV systolic and diastolic flow velocity ratios, the systolic fraction of PVFV and PVa velocity and duration. The results of this study point out limitations of the currently described methods, but also provide information that may improve their diagnostic accuracy or provide new variables for study. For instance, because peak PVa flow velocity and duration are influenced by respiration, these variables should be averaged over a number of beats or obtained at a standardized point in the respiratory cycle such as end-expiration apnea. Methods to correct for heart rate or the R-R interval if the diastolic velocity is above zero at the time of atrial contraction also need to be explored. The observation that increasing LA pressure results in a shortening of the Q-PVs2 interval suggests that new variables based on intervals that relate to LV filling pressures might be developed. Finally, how best to interpret transthoracic Doppler PV variables in the 70% of patients in whom the individual PVs1 and PVs2 flow components appear to be fused (45) should be investigated.

Study limitations. Because of difficulties in using sonomicrometer crystals with extensive hemodynamic instrumentation, LA and LV volume and contractility were not quantitated in these experiments. These would have provided insight into the relation of LA and LV compliance to the hemodynamic and Doppler changes observed and also would have allowed for a better analysis of the reservoir, conduit and booster pump functions of the LA. Other limitations include species differences in PVFV patterns between dogs and humans and the lack of information regarding how the findings would be altered in the presence of cardiac disease. As previously reported (10,12,43,44), healthy dogs have smaller PVa and PVs1 flow velocities and lower PV systolic to diastolic flow velocity ratios than seen in healthy young adults (24,27,28). Because baseline rest heart rates and filling pressures are similar in both species, it seems likely that LA and LV operating chamber compliance are lower in dogs.

Conclusions. Using the transesophageal pulsed wave Doppler technique, four PVFV components are identifiable and determined by PV–LA hemodynamic pressure gradients. These gradients appear to be influenced by a combination of physiologic events, which include RV stroke volume, the compliance of the pulmonary vasculature and LA and phasic changes in LA pressure. PV flow velocity components are significantly influenced by heart rate, respiration and LA pressure. These findings have implications for the interpretation of LV diastolic function and filling pressures by current Doppler echocardiographic techniques that require further clinical investigation.

I thank Becky Reinke for technical assistance and Mark Curry and Marvin Ruona for expert help in preparing the figures.

References

1. Lee G de J, Dubois AB. Pulmonary capillary blood flow in man. J Clin Invest 1955;43:1380–90.
2. Skalak R, Wiener F, Morkin E, Fishman A. The energy distribution in the pulmonary circulation. I: Theory. Phys Med Biol 1966;2:287–94.
3. Skalak R, Wiener F, Morkin E, Fishman A. The energy distribution in the pulmonary circulation. II: Experiments. Phys Med Biol 1966;3:437–49.
4. Wiener F, Morkin E, Skalak R, Fishman A. Wave propagation in the pulmonary circulation. Circ Res 1966;19:834–50.
5. Morkin E. Analysis of pulsatile blood flow and its clinical implications. N Engl J Med 1967;277:139–46.
6. Morkin E, Collins JA, Goldman HS, Fishman A. Pattern of blood flow in the pulmonary veins of the dog. J Appl Physiol 1965;20:1118–28.
7. Morgan BC, Abel FL, Mullins GL, Guntheroth WG. Flow patterns in cavae, pulmonary artery, pulmonary vein and aorta in intact dogs. Am J Physiol 1966;210:903–9.
8. Dixon S, Stanton N, Morrow AG. Pulmonary venous flow: the effects of alterations in left atrial pressure, pulmonary arterial occlusion and mitral regurgitation in the dog. Ann Surg 1971;174:944–9.
9. Kalmanson D, Toutain G, Novikoff N, Derai C. Retrograde catheterization of left heart cavities in dogs by means of an orientable directional Doppler-tipped flowmeter: a preliminary report. Cardiovasc Res 1972;6:309–18.
10. Smiseth OA, Lodemel K, Riddervold F, Blaha M. Changes in pulmonary vein flow pattern during volume loading. Cardiovasc Res 1993;21:1687–96.
11. Steen T, Voss BMR, Smiseth OA. Influence of heart rate and left atrial pressure on pulmonary venous flow pattern in dogs. Am J Physiol 1994;255: H2296–2302.
12. Hoit BD, Shao Y, Gabel M, Walsh Ra. Influence of loading conditions and contractile state on pulmonary venous flow: validation by Doppler velocimetry. Circulation 1992;86:651–9.
13. Hitch DC, Nolan SP. Descriptive analysis of instantaneous left atrial volume with special reference to left atrial function. J Surg Res 1981;30:110–20.
14. Hoit B, Ramrakhyani K. Pulmonary venous flow in cardiac tamponade: influence of left ventricular dysfunction and the relation to pulsus paradoxus. J Am Soc Echocardiogr 1991;4:559–70.
15. Nishikawa Y, Roberts JP, Tan P, Klopfenstein CE, Klopfenstein HS. Effect of dynamic exercise on left atrial function in conscious dogs. J Physiol 1994;481.2:457–68.
16. Skagseth E. Pulmonary vein flow pattern in man during thoracotomy. Scand J Thorac Cardiovasc Surg 1976;10:36–42.
17. Skagseth E. Pulmonary vein flow pattern in mitral incompetence: combined mitral stenosis/incompetence after prosthetic valve replacement. Scand J Thorac Cardiovasc Surg 1976;10:43–52.
18. Rajagopalan B, Friend J, Stallard T, de J Lee G. Blood flow in pulmonary veins: I. Studies in dog and man. Cardiovasc Res 1979;13:667–76.
19. Rajagopalan B, Friend A, Stallard T, de J Lee G. Blood flow in pulmonary veins: II. The influence of events transmitted from the right and left sides of the heart. Cardiovasc Res 1979;13:677–83.
20. Rajagopalan B, Bertram C, Stallard T, de J Lee G. Blood flow in pulmonary veins: III. Simultaneous measurements of their dimensions, intravascular pressure and flow. Cardiovasc Res 1979;13:684–92.
21. Keren G, Sherez J, Megedish R, Levitt B, Laniado S. Pulmonary venous flow pattern—its relationship to cardiac dynamics: a pulsed Doppler echocardiographic study. Circulation 1985;71:1105–12.
22. Keren G, Bier A, Sherez J, Miura D, Keefe D, LeJemtel T. Atrial

contraction is an important determinant of pulmonary venous flow. J Am Coll Cardiol 1986;7:693–5.
23. Smallhorn J, Greedom R, Olley P. Pulsed Doppler echocardiographic assessment of extraparenchymal pulmonary vein flow. J Am Coll Cardiol 1987;9:573–9.
24. Jiaen W, Youbin D, Ying W, Xinfang W. Pulmonary venous flow evaluated by Doppler echocardiography. Jpn Heart J 1989;30:55–63.
25. Schiavone W, Calafiore P, Salcedo E. Transesophageal Doppler echocardiographic demonstration of pulmonary venous flow velocity in restrictive cardiomyopathy and constrictive pericarditis. Am J Cardiol 1989;63:1286–8.
26. Bartzokis T, Lee R, Yeoh T, Grogin H, Schnittger I. Transesophageal echo-Doppler echocardiographic assessment of pulmonary venous flow patterns. J Am Soc Echocardiogr 1991;4:457–64.
27. Masuyama T, Lee J-M, Tamai M, Tanouchi J, Kitabatake A, Kamada T. Pulmonary venous flow velocity pattern as assessed with transthoracic pulsed Doppler echocardiography in subjects without cardiac disease. Am J Cardiol 1991;67:1396–1404.
28. Klein AL, Tajik AJ. Doppler assessment of pulmonary venous flow in healthy subjects and patients with heart disease. J Am Soc Echocardiogr 1991;4:379–92.
29. Arakawa M, Akamatsu S, Terazawa E, et al. Age-related increase in systolic fraction of pulmonary vein flow velocity–time integral from transesophageal Doppler echocardiography in subjects without cardiac disease. Am J Cardiol 1992;70:1190–4.
30. Oneglia C, Sabatini T, Rusconi C, Moretti R. Effect of aging on pulmonary venous flow velocity pattern: an echocardiographic Doppler study. Am J Noninvas Cardiol 1993;7:51–6.
31. Klein AL, Burstow DJ, Tajik AJ, Zachariah PK, Bailey KR, Seward JB. Effects of age on left ventricular dimensions and filling dynamics in 117 normal persons. Mayo Clin Proc 1994;69:212–24.
32. Nishimura RA, Abel MD, Hatle LK, Tajik AJ. Relation of pulmonary vein to mitral flow velocities by transesophageal echocardiography: effect of different loading conditions. Circulation 1990;81:1488–97.
33. Kuercherer HF, Muhiudeen IA, Kusumoto FM, et al. Estimation of mean left atrial pressure from transesophageal pulsed Doppler echocardiography of pulmonary venous flow. Circulation 1990;82:1127–39.
34. Basnight MA, Gonzalez MS, Kershenovich SC, Appleton CP. Pulmonary venous flow velocity: relation to hemodynamics, mitral flow velocity and left atrial volume and ejection fraction. J Am Soc Echocardiogr 1991;4:547–58.
35. Kuecherer H, Kusumoto F, Muhiudeen I, Cahalan M, Schiller NB. Pulmonary venous flow patterns by transesophageal pulsed Doppler echocardiography: relation to parameters of left ventricular systolic and diastolic function. Am Heart J 1991;122:1683–92.
36. Rossvoll O, Hatle LK. Pulmonary venous flow velocities recorded by transthoracic Doppler ultrasound: relations to left ventricular diastolic pressures. J Am Coll Cardiol 1993;21:1687–96.
37. Appleton CP, Galloway JM, Gonzalez MS, Gaballa M, Basnight MA. Estimation of left ventricular filling pressures using two-dimensional and Doppler echocardiography in adult cardiac patients: additional value of analyzing left atrial size, left atrial ejection fraction and the difference in the duration of pulmonary venous and mitral flow velocities at atrial contraction. J Am Coll Cardiol 1993;22:1972–82.
38. Brunazzi MG, Chirillo F, Pasqualani M, et al. Estimation of left ventricular diastolic pressures from precordial pulsed-Doppler analysis of pulmonary venous and mitral flow. Am Heart J 1994;128:293–300.
39. Hoffman T, Keck A, van Ingen G, Simic O, Ostermeyer J, Meinertz T. Simultaneous measurement of pulmonary venous flow by intravascular catheter Doppler velocimetry and transesophageal Doppler echocardiography: relation to left atrial pressure and left atrial and ventricular function. J Am Coll Cardiol 1995;26:239–49.
40. Cecconi M, Manfrin M, Zanoli R, Colonna P, Pangrazi A, Soro A. Doppler echocardiographic evaluation of left ventricular end-diastolic pressure in patients with coronary artery disease. J Am Soc Echocardiogr 1996;9:241–50.
41. Masuyama T, Lee J, Yamamoto K, Tanouchi J, Hori M, Kamada T. Analysis of pulmonary venous flow velocity patterns in hypertensive hearts: its complementary value in the interpretation of mitral flow velocity patterns. Am Heart J 1992;124:983–94.
42. Appleton CP, Hatle LK. The natural history of left ventricular filling abnormalities: assessment by two-dimensional and Doppler echocardiography. Echocardiography 1992;9:437–57.
43. Appleton CP, Gonzalez MS, Basnight MA. Relation of left atrial pressure and pulmonary venous flow velocities: importance of baseline mitral and pulmonary venous flow patterns studied in lightly sedated dogs. J Am Soc Echocardiogr 1994;7:264–75.
44. Hoit BD, Shao Y, Gabel M, Walsh R. In vivo assessment of left atrial contractile performance in normal and pathologic conditions using a time-varying elastance model. Circulation 1994;89:1829–38.
45. Jensen JL, Williams FE, Beilby BJ, et al. Feasibility of obtaining pulmonary venous flow velocity in cardiac patients using transthoracic pulsed wave Doppler technique. J Am Soc Echocardiogr 1997;10:60–6.
46. Appleton CP, Jensen JL, Hatle LK, Oh JK. Doppler evaluation of left and right ventricular diastolic function: a technical guide for obtaining optimal flow velocity recordings. J Am Soc Echocardiogr 1997;10:271–91.
47. Morkin E, Wiener F, Fishman A. Effects of breathing on pulmonary circulation. 7th Int Conf Med Biol Eng 1967:35–4.
48. Steen T, Kongsgaard E, Soyland E, Ihlen H. The influence of atrioventricular conduction and heart rate on the pulmonary venous flow pattern. J Am Soc Echocardiogr 1996;9:129–34.
49. Rakowski H, Appleton CP, Chan K-L, et al. Recommendations for the measurement and reporting of diastolic function by echocardiography. J Am Soc Echocardiogr 1996;9:736–60.
50. Oh JK, Appleton CP, Hatle LK, Nishimura RA, Seward JB, Tajik AJ. The noninvasive assessment of left ventricular diastolic function using two-dimensional and Doppler echocardiography. J Am Soc Echocardiogr 1997; 10:246–70.